Si diffusion path for pit-free graphene growth on SiC(0001)

G. F. Sun, Y. Liu, S. H. Rhim, J. F. Jia, Q. K. Xue, M. Weinert, and L. Li

Phys. Rev. B **84**, 195455 — Published 23 November 2011

DOI: 10.1103/PhysRevB.84.195455

A novel Si diffusion path for pit-free graphene growth on SiC(0001)

G. F. Sun[1, 2], Y. Liu[1], S. H. Rhim[1], J. F. Jia[3,4], Q. K. Xue[2, 3], M. Weinert[1], and L. Li[1*]

[1]Department of Physics and Laboratory for Surface Studies

University of Wisconsin, Milwaukee, WI 53211, USA

[2]Institute of Physics, Chinese Academy of Sciences, Beijing 100190, P. R. China

[3]Department of Physics, Tsinghua University, Beijing 100084, P. R. China

[4]Department of Physics, Shanghai Jiaotong University, Shanghai 200240, P. R. China

Abstract:

Density functional theory calculations reveal that the interfacial $6\sqrt{3}$x$6\sqrt{3}$ structure – a warped graphene layer with periodic inclusions of pentagon-hexagon-heptagon ($H_{5,6,7}$) defects – facilitates a novel Si diffusion path vertically through the interface layer during epitaxial growth of graphene on SiC(0001). The calculated diffusion barrier is 4.7 eV, competitive with Si interstitial diffusion of ~3.5 eV in SiC [M. Bockstedte, *et al.*, Phys. Rev. B **68**, 205201 (2003)]. Scanning tunneling microscopy study shows that for growth in an Ar background, where Si desorption is suppressed and all diffusion channels contribute, graphene films with reduced pit density can be grown on nominally flat SiC substrates. On the other hand, for Si diffusion-limited growth in ultrahigh vacuum, the Si interstitial diffusion is the energetically favorable path where the step edges serves as the necessary outlet towards Si desorption. The much higher density of step edges on vicinal substrates also facilitates the growth of pit-free graphene.

PACS: 81.05.ue, 61.48.Gh, 68.37.Ef, 68.35.Fx

*lianli@uwm.edu

Graphene is a sheet of sp^2 bonded carbon atoms with linear dispersion at the Dirac points, resulting in the extraordinary physical and electronic properties that have fueled the extensive research to explore their potential applications in optoelectronics[1]. Of particular interest is epitaxial graphene grown on SiC(0001) substrate, which provides wafer-sized material for large-scale device production[2]. Clearly different from the conventional vapor phase growth techniques such as molecular beam epitaxy[3], where nucleation and growth are controlled by surface adsorption, diffusion, and incorporation of adatoms that are supplied (typically) by thermal evaporation sources, the growth of epitaxial graphene arises from the thermal decomposition of SiC in vacuum, where the nucleation of new graphene layer from the liberated carbon atoms requires Si out-diffusion from the underlying SiC substrate and its subsequent desorption. To precisely control the number of graphene layers and to fabricate uniform films with high mobility, studies have been carried out to investigate the roles of SiC step instability[4], carbon adatom diffusion[5], and the effect of Ar or Si background pressure on the suppression of the Si desorption rate[2, 6]. Nevertheless, the atomic processes of the Si diffusion during growth are still largely unknown.

Previous studies have indicated that the growth of epitaxial graphene on the Si and C faces of SiC substrate are significantly different, indicating that the growth mechanisms are strongly dependent on the polarity of the starting substrate[7]. For graphene growth on the Si face SiC substrate, we show here that the atomic structure of the interfacial ($6\sqrt{3}$x$6\sqrt{3}$) (denoted "$6\sqrt{3}$" hereafter) layer that forms before 1st layer graphene growth plays a critical role in the growth kinetics, as Si atoms are no longer exposed for ready desorption after its formation. Consequently, the out-diffusion of Si likely takes two paths: either diffusing laterally in the SiC bulk to the step edges to desorb from there, or vertically pass through the $6\sqrt{3}$ interface layer to desorb from the surface. Our first-principles calculations show that the vertical path through the $6\sqrt{3}$ layer is facilitated by its unique structure with the periodic inclusions of pentagon-hexagon-heptagon ($H_{5,6,7}$)

defects[8], through which Si diffuses via a series of configurations involving the dissociation and formation of C-C and Si-C bonds. The calculated energy barrier for this novel path is 4.7 eV, making it energetically only slightly less favorable than the Si interstitial bulk diffusion[9-11] of ~3.5 eV. We further show that for growth in a background of Ar where Si desorption is suppressed and all diffusion channels contribute, graphene films with reduced pit density can be grown on nominally flat SiC substrates. On the other hand, for Si diffusion-limited growth, e.g., in ultrahigh vacuum (UHV), the much higher density of step edges readily available on vicinal substrates provides the necessary outlets for the energetically favorable lateral diffusion, and pit-free graphene can also be grown.

Experiments were carried out in an UHV chamber integrated with an Omicron variable-temperature STM[12]. The as-received nitrogen-doped 6H-SiC(0001) substrate was etched *ex situ* in H_2/Ar atmosphere at ~1600 ^oC first, then annealed in UHV in a Si flux (~0.1 ML/min) at 950 ^oC for 15 min to produce a (3x3) reconstructed surface, and then annealed at higher temperatures (1000-1300 ^oC) without Si flux for 10-20 min to grow graphene[13]. In addition, for growth in an Ar background pressure of 10^{-4} Torr, 10 sccm of Ar was introduced into the UHV chamber during growth.

The first-principles calculations, using the Full-potential Linearized Augmented Plane Wave (FLAPW) method as implemented in *flair*[14], model graphene using a 3x3 supercell, with a vacuum region of ~20 Å and a basis cutoff of ~195 eV. In order to model the Si diffusion path, the Si is moved in 0.125 Å steps relative to the buffer layer (defined by the vertical position of the carbon atom in the corner of the cell), allowing all other atomic coordinates to fully relax. This procedure mimics the dynamical process as a series of quasi-equilibrium steps, and allows for the breaking and reforming of chemical bonds. To address the effect of the substrate on the diffusion and the size of the overall self-diffusion barrier, additional relaxed calculations including two bilayers of SiC were done at several points along the diffusion path.

Figure 1 presents the progression of the surface morphology and atomic structure of the nominal flat SiC(0001) substrate at different stages of graphene growth in UHV. After growth at ~1000 ^{o}C (Fig. 1(a)), the morphology is characterized by terraces of ~200 nm separated by mostly steps of two bilayers (~5 Å). A close-up view of the structure on the terrace (Fig. 1(b)) shows a close-pack structure with a spacing of 0.52 nm, consistent with the (√3x√3)R30° assignment (denoted "√3" hereafter), which consists of a Si adatom at the T_4 site per unit cell[15]. Clearly visible are randomly distributed depressions (one circled) of different sizes, indicating desorption of Si adatoms at these sites.

At ~1100 ^{o}C, the step morphology is qualitatively similar (Fig. 1(c)), although two regions with low (*I*) and high (*II*) contrast are observed on the terrace. While atomic resolution imaging of region *I* shows the "√3" phase, a different structure that consists of two types of trimers pointing in opposite direction is observed in region *II*, as shown in Fig. 1(d). Close inspection of the image reveals an average spacing of ~19 Å, i.e., ~six times the lattice constant of the SiC(0001) surface. In addition, the population of up-pointing trimers could be up to 4 times more than that of the downward ones, depending on growth conditions[8]. Additional features (circled) are also observed in the region between these trimers, which has approximately (2x2) or (√3x√3) periodicity. These results indicate that region *II* is the interfacial (6√3x6√3) phase, consistent with earlier studies[16, 17]. Interestingly, a line profile across the two boundaries between the √3 and 6√3 phases (AA' in Fig. 1(e)) indicates a height difference of only 0.5-1.0 Å (depending on bias voltage), much less than that of a SiC bilayer step height of 2.5 Å, suggesting that the √3 and 6√3 are at the same layer.

First layer graphene begins to grow at ~1200 ^{o}C, accompanied also by step bunching (~six Si-C bilayers) and pit formation, as shown in Fig. 1(f). At this stage, the √3 region disappeared entirely, while the 6√3 structure can still be observed on ~5% of the surface (particularly at the bottom of the pits, as indicated by an arrow in Fig. 1(f)). The rest of the surface is converted to 1st layer graphene, as shown in Fig. 1(g). However, the main

features of the 6√3 layer are still visible; e.g., two representative features (marked by triangles and circle) are indistinguishable from those in Fig. 1(d), though not as sharp since they are now overlaid with a honeycomb lattice characteristic of the graphene. This behavior indicates that upon the growth of the 1st layer graphene, the 6√3 layer remains at the interface[18-21]. These structural evolutions at an atomic scale clearly indicate the growth of 1st layer graphene.

The close relationship between graphene morphologies and surface atomic structure suggests that upon the formation of the 6√3 layer that consists entirely of C, Si is no longer exposed for ready desorption, and hence Si out-diffusion becomes the rate-limiting step (given that for typical growth conditions in UHV Si desorption is fast). In particular, since the 6√3 phase proceeds immediately before the formation of the 1st layer graphene and remains at the interface, the atomic structure of this phase holds the key to unlock the growth kinetics of epitaxial graphene on Si-face SiC[6,22]. Our recent work has shown that the 6√3 interface is a warped graphene layer with periodic inclusions of pentagon-hexagon-heptagon ($H_{5,6,7}$) complexes covalently bonded to the Si atoms of the SiC(0001) substrate, as shown in Fig. 2(a)[8]. Because the insertion of pentagons and heptagons causes positive and negative curvatures in a honeycomb lattice[23,24], respectively, a free standing structure of this type is not energetically favored compared to a perfect honeycomb layer[8,25]. However, the warped layer becomes favorable when it is placed on SiC(0001) as it accommodates much better the Si-C bond distortion at the interface[8]. Upon the formation of this interfacial layer, further graphene growth requires Si diffusion to an exposed site to desorb. Two likely pathways are shown in Fig. 2(b): either vertically through the 6√3 layer to the surface (path 1), or laterally through the bulk to a step edge (path 2). Bulk Si diffusion typically involves multi-atoms and/or concerted mechanisms. Earlier studies have shown that the energy barrier for Si interstitial diffusion is ~3.5 eV[9-11]. (The barrier for bulk Si self-diffusion in SiC of ~9 eV[9-11] includes the energy for defect formation, i.e., the liberation of Si atom. Although this energy may be larger than that of

subsequent diffusion and desorption, it is common to both diffusion paths considered in this study; see below.)

For the vertical diffusion pathway through the 6√3 layer, our first-principles calculations indicate that it can also be an energetically competitive path for the out-diffusion of Si. The presence of the pentagon and heptagon of the $H_{5,6,7}$ defects facilitates the diffusion of the Si atom through a series of configurations involving the dissociation and formation of C-C and Si-C bonds. Snapshots of intermediate atomic steps at several heights of the Si atom relative to the surface are shown in Fig. 3, both in cross section (middle panel) and plane views (bottom panel). Initially, the Si atom, removed from the SiC substrate, diffuses upwards. At ~1.25 Å below the surface, the Si has diffused laterally to the heptagon, which begins to open up. At 0.5 Å below the surface, the Si moves toward the center of the heptagon, causing vertical displacements of the carbon atoms, and the formation of a Si-C bond with the C atom at the edge of the hexagon. As the Si further penetrates the heptagon, there are distortions and twisting of the C rings. The maximum barrier occurs between -0.25 and -0.125 Å, at which point the force on the Si atom also changes sign, i.e., indicating that it is being expelled to the other side. Energetically, the top of the barrier, which corresponds the coordinated relaxation of a large number of C atoms, is fairly flat (several tenths of an eV) over a range of ~0.5 Å in the Si vertical position. Although there are C atoms quite high above the Si for the "in-plane" configuration, they remain connected to the surface. As the Si starts to leave the buffer layer, the carbon atoms relax back towards a flat graphene layer[26]. The calculated barrier height is ~4.7 eV for this vertical diffusion path through the 6√3, much smaller than the barrier (>13 eV) for Si (or ~10 eV for He[27]) diffusion through a perfect honeycomb layer, making it energetically competitive with the alternative path for the disposal of Si. The reduced barrier for Si diffusion through the warped graphene layer is consistent with earlier calculations, where the penetration barriers of He atoms through

defected graphene layers have been found to decrease exponentially with the size of the defects[27].

Interactions with the substrate do not alter this overall picture: Relaxed calculations including the SiC substrate were done for the "top" configuration, and then for one of the Si atoms constrained at -1.25, -0.25, and 0 Å below the graphene sheet, as in Fig. 3; the horizontal positions of the Si atom were allowed to relax. (The C atoms in the graphene layer, as well as all other atoms in the upper SiC bilayer, were allowed to fully relax.) From these calculations, the calculated overall self-diffusion barrier – the combination of liberation and diffusion barriers – was found to be ~7.9 eV, comparable to the experimental[9] and theoretical[10] values of 7.2-9.5 and ~9 eV, respectively. The difference between the Si at -0.25 Å (7.8 eV relative to the ground state configuration, and slightly before the maximum of barrier) and for Si in-plane (7.4 eV, where the force on the Si is pushing it out of the surface) is essentially unchanged, while the value at -1.25 Å (4.8 eV) is slightly lower than the 5.1 eV expected from combining the values in Fig. 3 and the ~7.9 eV total barrier. This decrease of the barrier for the Si near the substrate (compared to that calculated for the isolated layer) is due to the Si at this height being closer to the substrate than the graphene (nominally 2.3 Å above the substrate) and still having significant bonding to the surface; as the Si moves up, this bonding decreases and the barrier is dominated by the strong in-plane bonding of the graphene buffer layer. Thus, the total (liberation/formation plus migration) barrier for this process is comparable to the corresponding barrier in the bulk even though the diffusion barrier through the buffer layer is slightly larger than the bulk interstitial migration barrier. (The formation energy for a surface Si vacancy is several eV less than for a bulk one because fewer bonds need to be broken, favoring a surface process.)

The availability of the two diffusion pathways has direct consequence for the epitaxial graphene growth on SiC(0001). By tweaking the growth conditions, one can carry out the growth in a desorption-limited regime where both diffusion paths are

relevant, or in a diffusion-limited regime, where the diffusion path with the lowest energy barrier dominates. For typical graphene growth at ~1200 ^{o}C in UHV, any exposed Si readily desorbs from the surface, and therefore diffusion is the rate-limiting step. Hence the Si interstitials bulk diffusion towards step edges is the preferred pathway for Si out-diffusion, where step edges provide the necessary outlet for its subsequent desorption.

On a nominally flat substrate, steps are relative scarce. Step edges can be created, however, when pits are formed in the growth process, as shown above in Fig. 1(f). Several factors could contribute to pit formation. First, our results and others[22] have shown that the √3 and 6√3 phases coexist on the same terrace at the initial stages of growth. Second, further growth of the √3 layer into the 6√3 requires additional C atoms to be liberated from the decomposition of Si-C bilayers. Our calculations indicate a larger energy barrier for Si vertical diffusion through the 6√3, suggesting that Si desorption from this area is much slower than that from the √3, therefore the growth from 6√3 to form graphene is impeded[22], and the growth is dominated by the conversion of √3 regions into 6√3 at the intermediate stages. The later process proceeds via the disposal of Si atoms liberated from 3 Si-C layers, therefore resulting in the formation of a pit of ~0.8 nm in depth. Note that while the decomposition of subsurface Si-C occurs in all areas, due to the higher energy barrier for Si diffusion through the 6√3 layer (which facilitates the forward reaction), the reverse reaction of the recombination of Si and C back to form Si-C would also occur at a comparable rate in the 6√3 regions. Finally, the evolution of the 6√3 into 1st layer graphene requires additional liberated C atoms, which results in deepening of the pit, with the structure at the bottom of the pit always be the 6√3 at these intermediate stages (Fig. 1(f)). The step edges associated with these pits, can serve as additional outlets for the Si desorption. As growth proceeds, the formation of pits escalates, and depths of a few nm often have been observed, leading to surface roughening and spatial variation in graphene thickness, which in turn likely contributes to the reduced carrier mobility commonly found on graphene films grown on SiC(0001).

The question arises then: can pit-free graphene be grown on vicinal substrates where steps are abundantly available? STM images of graphene growth on a 3.5^{o} miscut SiC(0001) substrate are shown in Fig. 4. Starting from the Si-rich (3x3) with ~ 1ML Si coverage (Fig. 4(a)) where steps are mostly three SiC bilayers, Si desorption leads to the less Si-rich √3 with ~ 1/3 ML Si, where steps are bunched into ~ 6 bilayers (Fig. 4(b)). Interestingly, once the 6√3 structure begins to form, the motion of the steps is also pinned. The steps in between, however, debunch, and the terraces become narrower, i.e., the diffusion length for Si to reach the step edges is shortened (Fig. 4(c)). These results indicate SiC step edges play critical role in facilitating Si desorption[28-34]. Finally, as graphene grows on top of the 6√3, due to the pinning of the steps, larger terraces grow at the expense of smaller ones, resulting in greater step bunching (~twelve Si-C bilayers), as shown in Fig. 4(d), where pit-free graphene is grown.

On the other hand, in the case of graphene growth in a Si flux or in an Ar ambient, desorption of Si is significantly reduced and the growth becomes desorption-limited[2, 6]. Here all diffusion paths become relevant, i.e., the vertical diffusion through the 6√3 layer, although slightly higher in energy, can become an important competing mechanism. Since this diffusion path leads to desorption from the surface, step edges are no longer crucial. In addition, the suppression of Si desorption would slow down growth of the √3 phase to the 6√3 layer, and therefore significantly suppress the pit formation. Hence even on flat substrates where steps are sparse, graphene films with very few pits have also been grown in the presence of Si fluxes in UHV[6], or in Ar ambient[2].

We have also grown graphene on SiC(0001) in an Ar background of 10^{-4} Torr in UHV at ~1300 ^{o}C on a flat substrate, as shown in Fig. 5. A much more uniform film with a honeycomb structure similar to that of Fig. 1(g) is observed on the terrace (indicative of the 1st layer graphene), with pits only ~ 1 or 2 SiC bilayers deep and a density of ~5x10^{7} cm^{-2}, one order of magnitude less than that of graphene grown without Ar. The observation of only the 1st layer graphene is consistent with an earlier study[2], suggesting

self-limited growth. Step bunching with wavy step edge profiles is also observed, which may be related to carbon diffusion[5].

In summary, we have investigated Si diffusion pathways during the epitaxial growth of graphene on Si-face SiC (0001) substrate. Based on first-principles calculations, we find a novel vertical diffusion through the 6√3x6√3 structure with a barrier of ~4.7 eV (~7.9 eV for the total self-diffusion barrier), which is energetically slightly less favorable than Si interstitial diffusion in the SiC bulk. This mechanism explains the experimental observations that when Si diffusion is the rate limiting step, as typically the case in most growth in UHV, pits formation are prevalent since lateral bulk diffusion to a step edge for desorption is favored. On vicinal substrates where steps are abundantly available, pit-free graphene can be grown. On another hand, when Si desorption is limited, such as in the case of growth in an Ar or Si background, all diffusion pathways can become relevant, i.e., vertical diffusion through the 6√3 layer becomes an important competing mechanism, such that even on flat substrates where steps are scarce, graphene with few pits can be grown. These results provide insights into the effect of the interplay between diffusion and desorption on the self-limiting growth mechanism of epitaxial growth of graphene on SiC(0001) that is poised to impact the development of next generation electronics.

Acknowledgment: This work was supported by DOE (DE-FG02-07ER46228). JFJ and QKX acknowledge supports from NSFC and MOST.

Figures captions:

Fig. 1 (Color online) Topography images showing the evolution of the step morphology and surface structure during epitaxial growth of graphene on 6H-SiC(0001) as a function of temperature: (a) morphology at 1000 ^{o}C (1.0x1.0 μm^2, V_s=-1.4 V, I_t=1.2 nA); (b) atomic resolution image of the ($\sqrt{3}$ x $\sqrt{3}$)R30° structure (1.0x1.0 μm^2, V_s=-1.4 V, I_t=1.2 nA). Circled is a randomly distributed depression forms after the desorption of Si adatoms; (c) morphology at 1100 ^{o}C (1.0x1.0 μm^2, V_s=-2.0 V, I_t=0.5 nA.); (d) atomic resolution image of the ($6\sqrt{3}$ x $6\sqrt{3}$)R30° structure (0.5x0.5 μm^2, V_s=-1.4 V, I_t=1.2 nA). The triangles and circle highlights the characteristic features found on the ($6\sqrt{3}$ x $6\sqrt{3}$)R30° surface (see details in the text); (e) STM images of the coexisting phases of ($\sqrt{3}$ x $\sqrt{3}$)R30° and ($6\sqrt{3}$ x $6\sqrt{3}$)R30° (50x60 nm^2, V_s=-1.6 V, I_t=1.2 nA), and line profile along AA'; (f) morphology at 1200 ^{o}C (1x1 μm^2, V_s=-1.6 V, I_t=1.2 nA). Black arrow indicates a pit structure on the surface; (g) atomic resolution image of the 1st layer graphene where the $6\sqrt{3}$ interface layer is still visible (50x50 nm^2, V_s=-1.4 V, I_t=1.2 nA). The triangles and circle highlight the characteristic features found on 1st layer graphene (see details in the text).

Fig. 2 (Color online) (a) Ball-and-stick model of the warped graphene model for the ($6\sqrt{3}$ x $6\sqrt{3}$) interface structure with the periodic inclusions of $H_{5,6,7}$ defects. (b) Ball-and-stick model illustrating possible diffusion paths for Si during epitaxial growth: 1) vertical diffusion through the warped interfacial layer, and 2) lateral bulk diffusion towards step edges.

Fig. 3 (Color online) Energies (top panel) and snapshots of the vertical migration process of Si through the $6\sqrt{3}$ layer in cross section (middle panel) and plane (bottom panel) view. The energies are calculated with respect to the total energy of an interstitial Si atom and the graphene layer with the $H_{5,6,7}$ defect.

Fig. 4 (Color online) STM images of the evolution of the step morphology on a vicinal 6H-SiC(0001) substrate as a function of temperature, when the surface changes from (a) (3x3) at 900 ^{o}C, V_s=-3.8V, I_t=0.2nA; to (b) ($\sqrt{3}$x$\sqrt{3}$) at 1000 ^{o}C, V_s=-6.8V, I_t=0.3nA; to (c) ($6\sqrt{3}$x$6\sqrt{3}$) + disordered phases at 1050 ^{o}C, V_s=-3.3V, I_t=0.1nA; to (d) ($6\sqrt{3}$x$6\sqrt{3}$) + 1st layer graphene at 1100 ^{o}C, V_s=-3.1V, I_t=0.1nA. Image sizes are (0.5x0.5) μm^2 for all.

Fig.5 STM image of graphene grown in 10^{-4} Torr of Ar at 1300 ^{o}C (2.0x2.0 μm^2, V_s=-1.6 V, I_t=1.2 nA).

References:

[1] Y.-M. Lin, C. Dimitrakopoulos, K. A. Jenkins, D. B. Farmer, H.-Y. Chiu, A. Grill, and P. Avouris, Science **327**, 662 (2010).

[2] K. V. Emtsev, et al., Nat Mater **8**, 203 (2009).

[3] L. L. Chang and K. Ploog eds., *Molecular beam epitaxy and heterostructures* (Springer, 1985).

[4] V. Borovikov and A. Zangwill, Physical Review B **80**, 121406 (2009).

[5] T. Ohta, N. C. Bartelt, S. Nie, K. Thurmer, and G. L. Kellogg, Physical Review B **81**, 121411 (2010).

[6] R. M. Tromp and J. B. Hannon, Physical Review Letters **102**, 106104 (2009).

[7] J. Hass, W. A. de Heer, and E. H. Conrad, Journal of Physics: Condensed Matter **20**, 323202 (2008).

[8] Y. Qi, S. H. Rhim, G. F. Sun, M. Weinert, and L. Li, Physical Review Letters **105**, 085502 (2010).

[9] J.D. Hong, M.D. Hon, and R.F. Davis, Ceram. Int. **5**, 155 (1979); M.H. Hon, R.F. Davis, and D.E. Newbury, J. Mater. Sci. **15**, 2073 (1980); J.D. Hong and R.F. Davis, J. Am. Ceram. Soc. **63**, 546 (1980); J.D. Hong, R.F. Davis, and D.E. Newbury, J. Mater. Sci. **16**, 2485 (1981).

[10] M. Bockstedte, A. Mattausch, and O. Pankratov, Physical Review B **68**, 205201 (2003).

[11] M. Bockstedte, A. Mattausch, and O. Pankratov, Physical Review B **69**, 235202 (2004).

[12] Y. Cui and L. Li, Physical Review B **66**, 155330 (2002).

[13] G. F. Sun, J. F. Jia, Q.-K. Xue, and L. Li, Nanotechnology **20**, 355701 (2009).

[14] M. Weinert, G. Schneider, R. Podloucky, and J. Redinger, Journal of Physics: Condensed Matter **21**, 084201 (2009).

[15] J. E. Northrup and J. Neugebauer, Physical Review B **52**, R17001 (1995).

[16] F. Owman and P. Martensson, Surface Science **369**, 126 (1996).

[17] C. Riedl, U. Starke, J. Bernhardt, M. Franke, and K. Heinz, Physical Review B **76**, 245406 (2007).

[18] G. M. Rutter, N. P. Guisinger, J. N. Crain, E. A. A. Jarvis, M. D. Stiles, T. Li, P. N. First, and J. A. Stroscio, Physical Review B **76**, 235416 (2007).

[19] K. V. Emtsev, F. Speck, T. Seyller, L. Ley, and J. D. Riley, Physical Review B **77**, 155303 (2008).

[20] P. Lauffer, K. V. Emtsev, R. Graupner, T. Seyller, L. Ley, S. A. Reshanov, and H. B. Weber, Physical Review B **77**, 155426 (2008).

[21] F. Varchon, P. Mallet, J. Y. Veuillen, and L. Magaud, Physical Review B **77**, 235412 (2008).

[22] J. B. Hannon and R. M. Tromp, Physical Review B **77**, 241404 (2008).

[23] J.-C. Charlier and G.-M. Rignanese, Physical Review Letters **86**, 5970 (2001).

[24] S. Ihara, S. Itoh, K. Akagi, R. Tamura, and M. Tsukada, Physical Review B **54**, 14713 (1996).

[25] E. Cockayne, G. M. Rutter, N. P. Guisinger, J. N. Crain, P. N. First, and J. A. Stroscio, Physical Review B **83**, 195425 (2011).

[26] At high temperatures (or when the $6\sqrt{3}$ layer becomes untethered/unstable as the Si diffuses away), some fraction of the C atoms that are displaced high above the plane (e.g.., Fig. 3, "in-plane") may also leave the surface. Thus, the vertical Si diffusion may trigger a nucleation event to locally transform the $H_{5,6,7}$ defect (with its two extra C atoms) into the regular graphene honeycomb structure. A discussion of the full dynamics, including the energy dependence of the diffusion barrier on the Si concentration in the interface region, is beyond the scope of this paper.

[27] O. Leenaerts, B. Partoens, and F. M. Peeters, Applied Physics Letters **93**, 193107 (2008).

[28] J. Penuelas, A. Ouerghi, D. Lucot, C. David, J. Gierak, H. Estrade-Szwarckopf, and C. Andreazza-Vignolle, Physical Review B **79**, 033408 (2009).

[29] C. Virojanadara, Syv, auml, M. jarvi, R. Yakimova, L. I. Johansson, A. A. Zakharov, and T. Balasubramanian, Physical Review B **78**, 245403 (2008).

[30] H. Huang, W. Chen, S. Chen, and A. T. S. Wee, ACS Nano 2, 2513 (2008).

[31] M. Hupalo, E. H. Conrad, and M. C. Tringides, Physical Review B **80**, 041401 (2009).

[32] M. L. Bolen, S. E. Harrison, L. B. Biedermann, and M. A. Capano, Physical Review B **80**, 115433 (2009).

[33] S. Tanaka, K. Morita, and H. Hibino, Physical Review B **81**, 041406 (2010).

[34] J. Borysiuk, R. Bozek, W. Strupinski, A. Wysmolek, K. Grodecki, R. Steapniewski, and J. M. Baranowski, Journal of Apply Physics **105**, 023503 (2009).

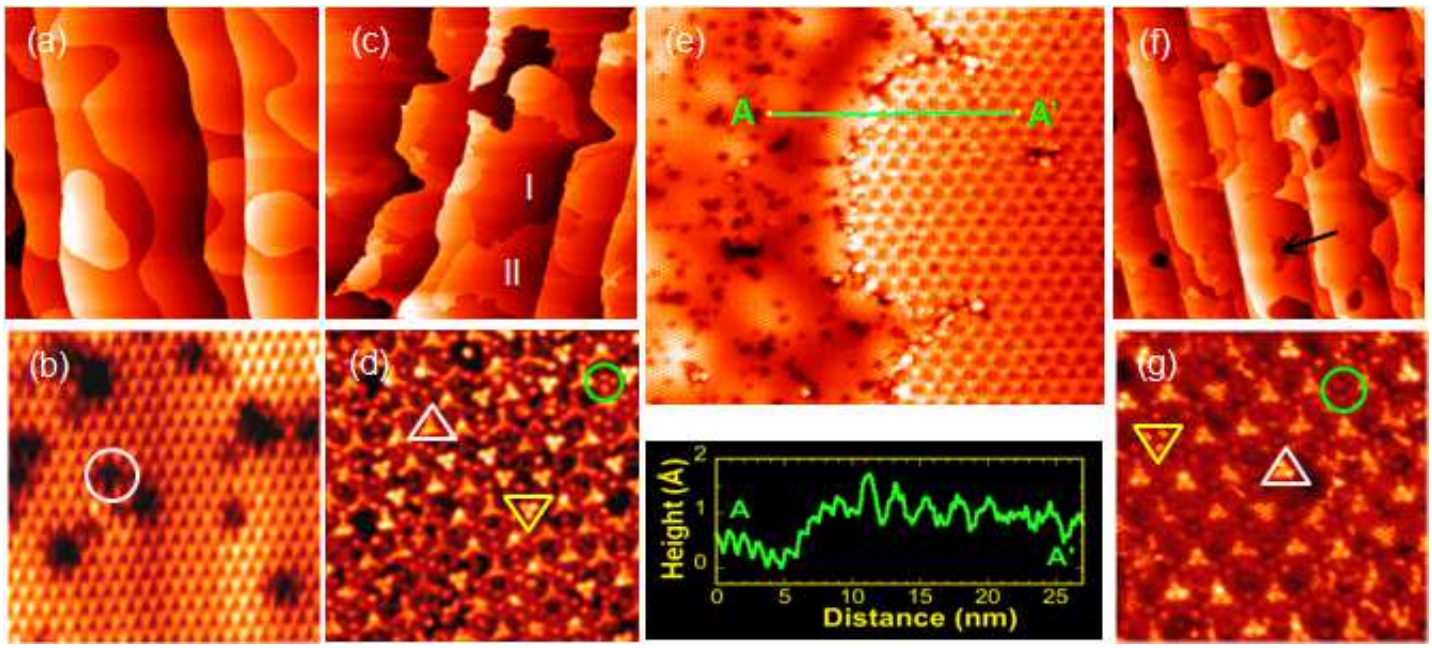

Figure 1 XF10018B 28OCT2011

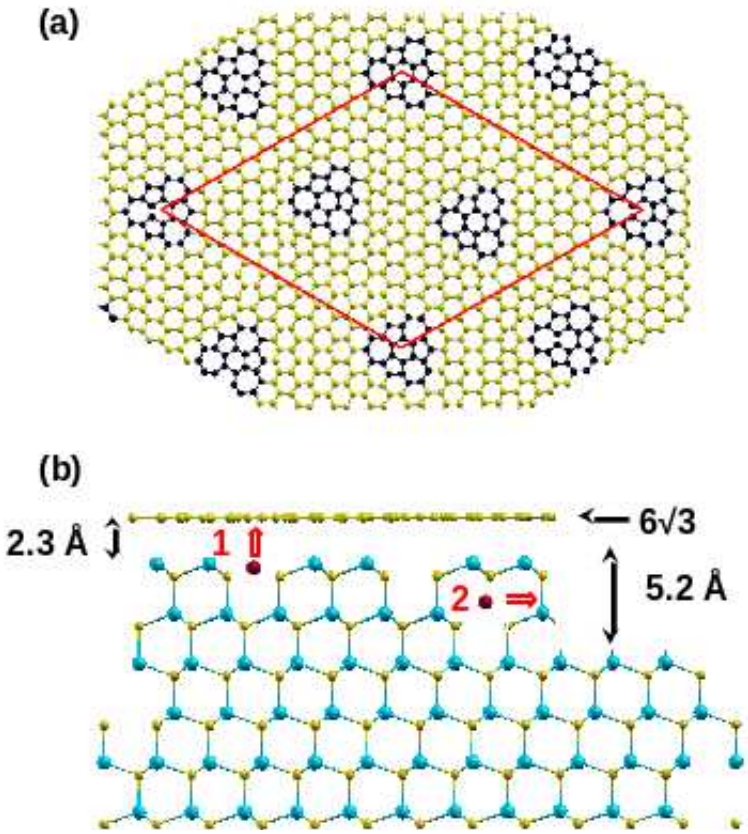

Figure 2 XF10018B 28OCT2011

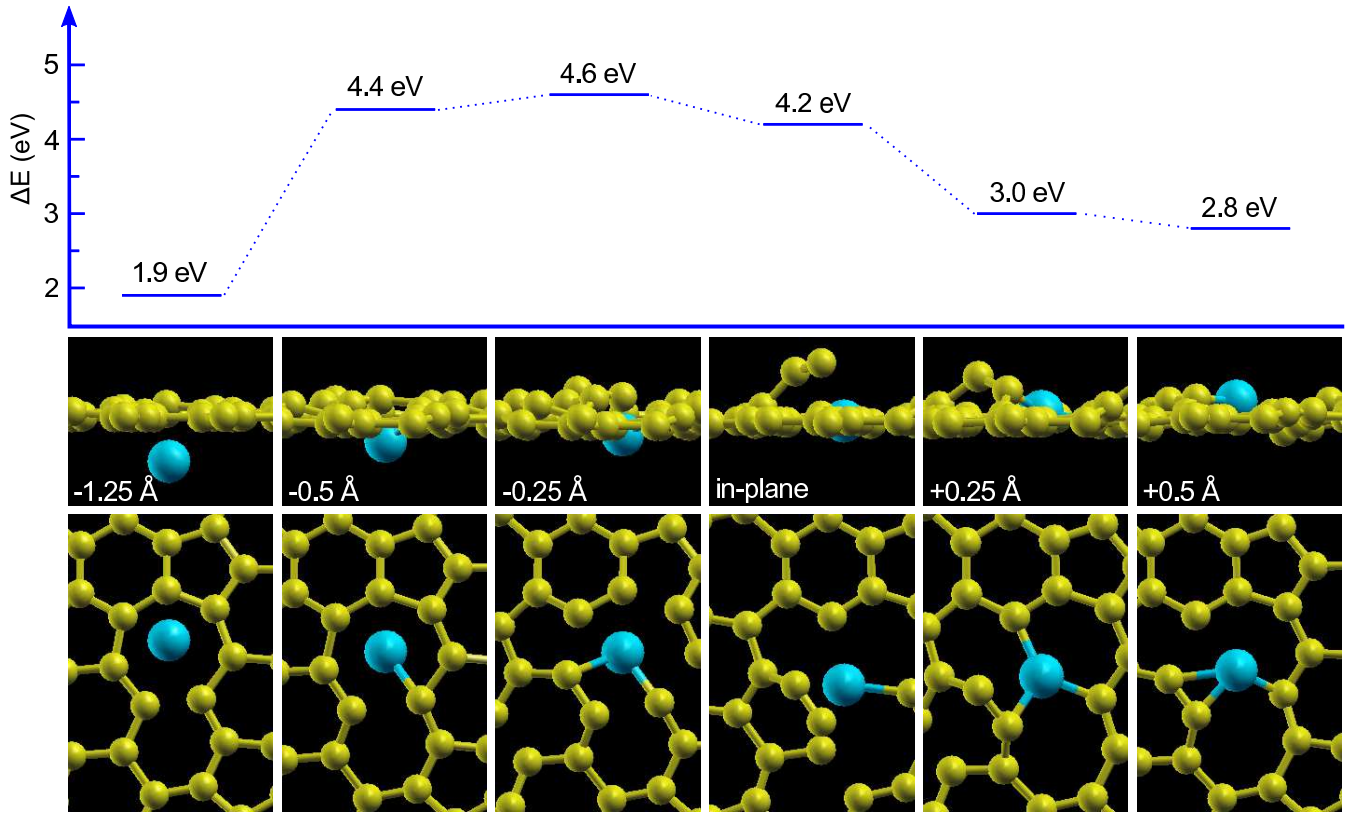

Figure 3 XF10018B 28OCT2011

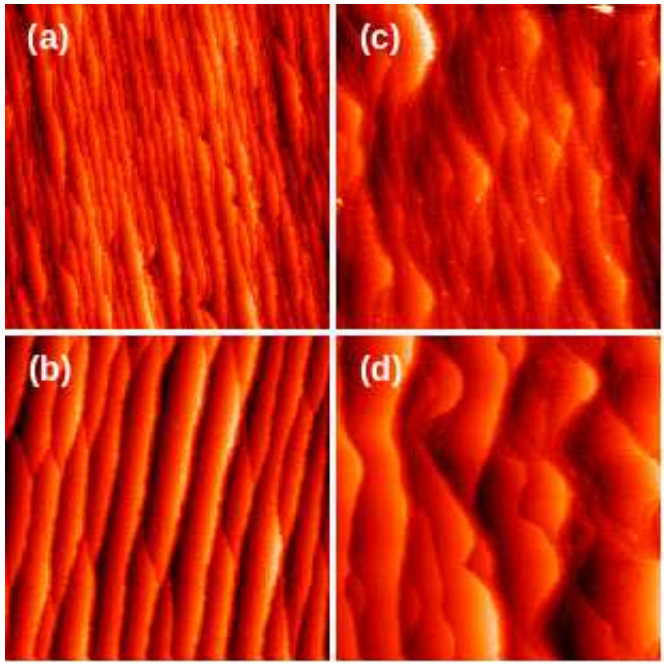

Figure 4 XF10018B 28OCT2011

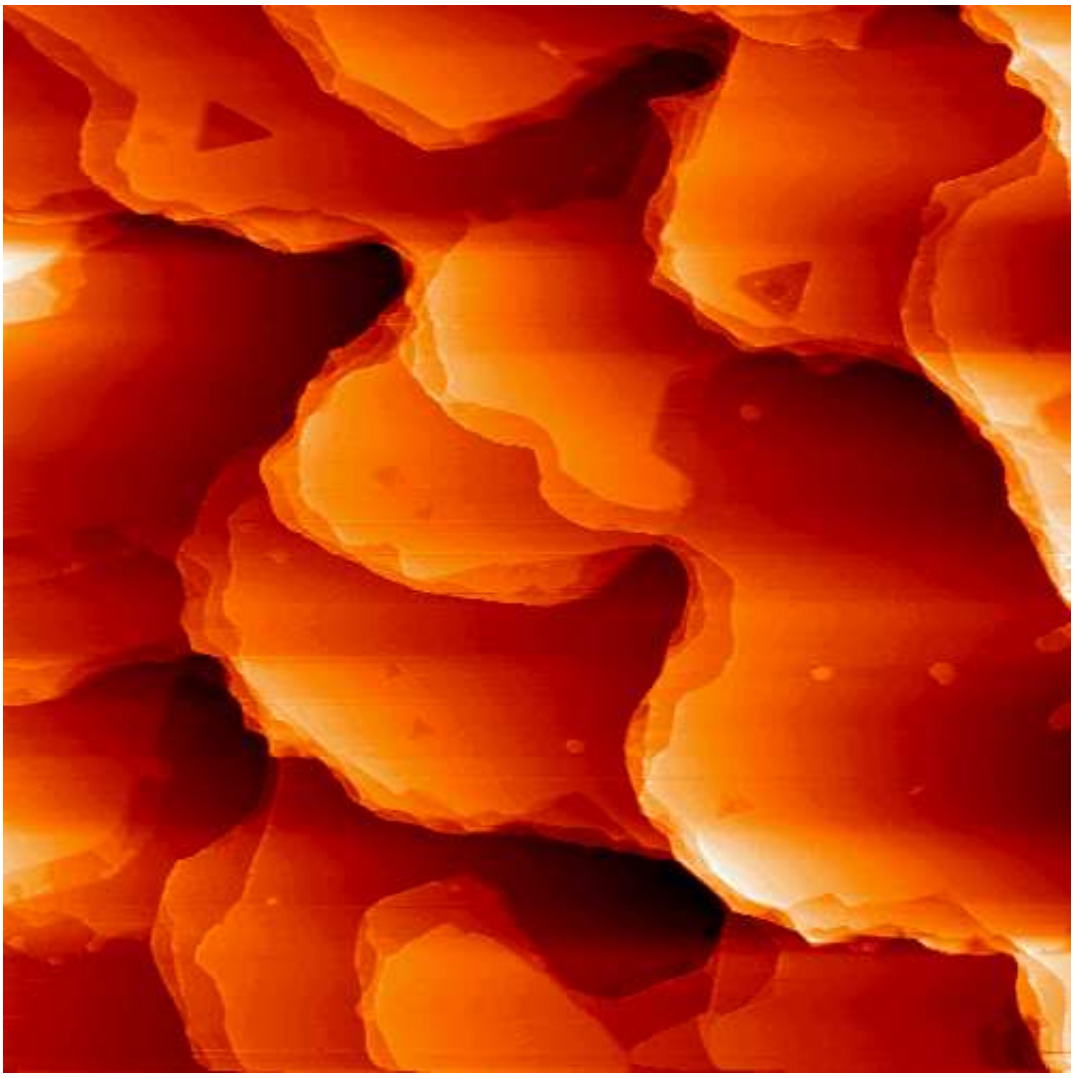

Figure 5 XF10018B 28OCT2011